

## INFLUENCE OF HEAT TREATMENT ON THE STRUCTURAL AND MAGNETIC CHARACTERISTICS OF $(\text{Nd}_x\text{Pr}_{1-x})_2\text{Fe}_{14}\text{B}$ -BASED MAGNETIC MATERIAL FOR LOW-TEMPERATURE APPLICATION

Received – Prispjelo: 2015-11-06

Accepted – Prihvaćeno: 2016-03-10

Original Scientific Paper – Izvorni znanstveni rad

Sintered Pr-Nd-Fe-B-based permanent magnets with 10 and 13 wt. % of Pr were prepared by traditional technology and then subjected to various heat treatments. Stoichiometric composition of the matrix grains corresponds to  $(\text{Pr}_{0.3}\text{Nd}_{0.7})_2\text{Fe}_{14}\text{B}$  and  $(\text{Pr}_{0.4}\text{Nd}_{0.6})_2\text{Fe}_{14}\text{B}$  compounds, respectively. Conducted thermomagnetic analysis to samples of these magnets showed the presence of spin-reorientation transition in temperature 95 and 75 K, respectively. This makes the magnet potentially applicable for low temperatures. For these compounds, we have determined the optimum heat-treatment conditions. The magnetic domain structure of the magnet subjected to an optimum heat treatment has been studied. The effect of different low-temperature heat treatments on the magnetic properties of magnets has been demonstrated.

*Key words:* Nd-Pr-Fe-B magnet, optimum heat treatment, spin-reorientation transition, domain structure

### INTRODUCTION

In recent years, the Nd-Fe-B-based magnetic materials attracted high interest due to their possible application even at cryogenic temperatures [1]. The low-temperature application of magnets based on non-alloyed  $\text{Nd}_2\text{Fe}_{14}\text{B}$  compound is limited by the existence of spin-reorientation transition (SRT) at 135 K, which is accompanied by a decrease in hysteretic characteristics of magnets [2]. The partial substitution of praseodymium for neodymium (which forms continuous solid solutions) in the magnetic  $(\text{Nd}_x\text{Pr}_{1-x})_2\text{Fe}_{14}\text{B}$  alloys for Nd-Fe-B-based permanent magnets allows us to decrease the SRT temperature due to the absence of transition of the  $\text{Pr}_2\text{Fe}_{14}\text{B}$  compound [2]. Thus, the complete substitution of Pr for Nd allows the SRT to be eliminated up to 4,2 K. Moreover, it is known [3, 4] that the substitution of praseodymium for neodymium allows us to increase substantially the magnetization coercive force ( $H_{cj}$ ).

This is related to the higher magnetic anisotropy field for the  $\text{Pr}_2\text{Fe}_{14}\text{B}$  compound (7,2 MA/m) as compared to that for the  $\text{Nd}_2\text{Fe}_{14}\text{B}$  compound (5,6 MA/m) [2]. The compounds have a tetragonal crystal structure with a strong magneto-crystalline anisotropy oriented along the crystallographic  $c$  axis [001]. In the case of

substitution of Pr for Nd, the other hysteretic parameter, saturation magnetization, can be almost unchanged ( $B_s$  for  $\text{Nd}_2\text{Fe}_{14}\text{B}$  and  $\text{Pr}_2\text{Fe}_{14}\text{B}$  is 1,6 and 1,5 T, respectively [2]). This fact determines the possibility of designing the high-efficiency high-coercive permanent magnets for low-temperature applications.

According to literature data [5] on the compositional dependence of the spin-reorientation transition temperature for the  $(\text{Nd}_{1-x}\text{Pr}_x)_2\text{Fe}_{14}\text{B}$  system, the substitution of Pr atoms for the half of Nd atoms allows us to decrease the spin-reorientation transition temperature to 75 K, i.e., below the liquid nitrogen temperature.

Several publications about the Nd-Fe-B-based magnets for cryogenic application include those presented at the REPM-2008 conference by Vacuumschmelze GmbH [6] ( $(\text{Pr}_{0.8}\text{Nd}_{0.2})_2\text{Fe}_{14}\text{B}$  magnets do not undergo the spin reorientation of the 2-14-1 phase at ~140 K and reach a remanence of 1,62 T at 77 K) and by Hitachi ( $\text{Pr}_2\text{Fe}_{14}\text{B}$  compositions), and at the REPM-2014 conference only by Vacuumschmelze GmbH [7]. The VA-CODYM 131 DTP grade magnets [7] were developed, in which the coercivity at room temperature was increased by the grain-boundary diffusion treatment with Tb. The following characteristics have been reached  $H_{cj} = 1\,800$  kA/m and  $B_r = 1,41$  T at 293 K and  $H_{cj} = 6\,300$  kA/m and  $B_r = 1,62$  T at 77 K.

The effect of heat treatment on the magnets having the analogous composition  $(\text{Nd,Pr(Tb,Dy,Gd)}-(\text{Fe,Co,Al,Cu})\text{-B})$  magnets was studied in [8]. The magnet was heat treated in two different ways and investigated in the temperature range from 4,2 to 400 K. After an opti-

K. Skotnicová, T. Čegan, D. Růžička, O. Životský, K. Hrabovská, RMSTC, FMME, VŠB-TU Ostrava, Czech Republic. G.S. Burkhanov, N.B. Kolchugina, TEKHMA Co Ltd., Moscow, Russia. Y.S. Koshkid'ko, J. Cwik, International Laboratory of High Magnetic Fields and Low Temperatures, PAS, Wrocław, Poland. A.A. Lukin, JSC SPETSMAGNIT, Moscow, Russia.

mal heat treatment, the magnetization coercive force  $H_{cj} = 1\,640$  and  $5\,040$  kA/m for room temperature and  $10\text{ K}$  was obtained.

The aim of the present study is to determine the optimum heat-treatment conditions for the sintered permanent magnets based on the  $(\text{Nd}_x\text{Pr}_{1-x})_2\text{Fe}_{14}\text{B}$  system and to study their structure and magnetic hysteretic properties.

## EXPERIMENTAL

The chemical composition of sintered magnets, which were prepared by traditional powder technology [9-11], is given in Table 1.

Table 1 The chemical composition of sintered magnets in / wt. %.

| Sample  | Nd | Pr | Ti  | Al  | Cu  | B   | Fe   |
|---------|----|----|-----|-----|-----|-----|------|
| N1 – N3 | 23 | 10 | 0,9 | 0,4 | 0,2 | 1,3 | bal. |
| N4      | 23 | 13 | 0,9 | 0,4 | 0,2 | 1,3 | bal. |

Starting alloys were melted using a Balzers VSG vacuum induction furnace and subsequently cast onto a copper water-cooled mould. Ingots were subjected to hydrogen decrepitation and subsequently to milling in a vibratory mill with an isopropyl alcohol medium. Powders were compacted at the pressure of  $30\text{ MPa}$  in a textured magnetic field of  $1,6\text{ T}$ . Magnet blanks were sintered in vacuum at the temperatures from  $1\,080$  to  $1\,100\text{ °C}$ . The following heat treatments were performed: a)  $500\text{ °C}$ ,  $2\text{ h}$  +  $475\text{ °C}$ ,  $0,5\text{ h}$  +  $400\text{ °C}$ ,  $20\text{ h}$  (sample N1); b)  $500\text{ °C}$ ,  $2\text{ h}$  (sample N2 and N4); and c)  $500\text{ °C}$ ,  $2\text{ h}$  +  $900\text{ °C}$ ,  $2\text{ h}$  (sample N3). Magnetic properties of magnets were studied at room temperature in magnetic fields of to  $12\text{ MA/m}$  using a MN-50 hysteresigraph and a closed magnetic circuit. Samples were preliminary magnetized in pulsed magnetic fields of up to  $12\text{ MA/m}$ .

Thermal magnetic analysis of permanent magnet samples was performed by measuring temperature dependences of magnetization in a low magnetic field. A vibrating-sample magnetometer was used. The magnetic field was applied along the magnetic texture axis of magnet.

The high-resolution field emission gun-scanning electron microscope QUANTA 450 FEG equipped with an energy dispersive X-ray analyser APOLLO X (SEM/EDX) was applied for the investigation of microstructure and phase chemical composition of magnets. Specially designed Zeiss microscope was used to visualize the magnetic domain patterns on the surface of magnetic materials using the magneto-optical Kerr microscopy. Domains were observed at low magnetic fields (practically in remanent state).

## RESULTS AND DISCUSSION

Data on the magnetic hysteretic properties of the studied magnets are given in Table 2. It is evident that

Table 2 Hysteretic properties\* of magnets subjected to different heat treatments.

| Sample | $H_{cj}$ / kA/m | $H_k$ / kA/m | $B_r$ / T | $(BH)_{max}$ / kJ/m <sup>3</sup> |
|--------|-----------------|--------------|-----------|----------------------------------|
| N1     | 810             | 580          | 1,25      | 296                              |
| N2     | 1 264           | 1 248        | 1,25      | 302                              |
| N3     | 1 000           | 990          | 1,25      | 296                              |
| N4     | 1 166           | 1 143        | 1,27      | 311                              |

\*Note:  $H_{cj}$  is the magnetization coercive force;  $H_k$  is the critical field (magnetization reversing field, at which 10 % decrease in the magnetization (with respect to the residual induction) takes place);  $B_r$  is the residual magnetic induction; and  $(BH)_{max}$  is the maximum energy product.

the heat treatment at  $500\text{ °C}$  for  $2\text{ h}$  (samples N2 and N4) allowed us to reach the high hysteretic properties. The subsequent heat treatments at both lower and higher temperatures resulted in the decrease of the coercive force of magnets.

The microstructure of magnets with 10 and 13 wt. % Pr taken with SEM is documented in Figure 1. The results of chemical analysis of magnets are summarized in Table 3. The phases found in the magnet structure can be identified as the main magnetic  $(\text{Nd,Pr})_2\text{Fe}_{14}\text{B}$  phase (point 1),  $(\text{Nd,Pr})_{1,1}\text{Fe}_4\text{B}_4$  phase (point 2),  $(\text{Nd,Pr})_{rich}$  phase observed at grain boundaries (point 3),  $\text{Nd}(\text{Pr})\text{O}$ ,

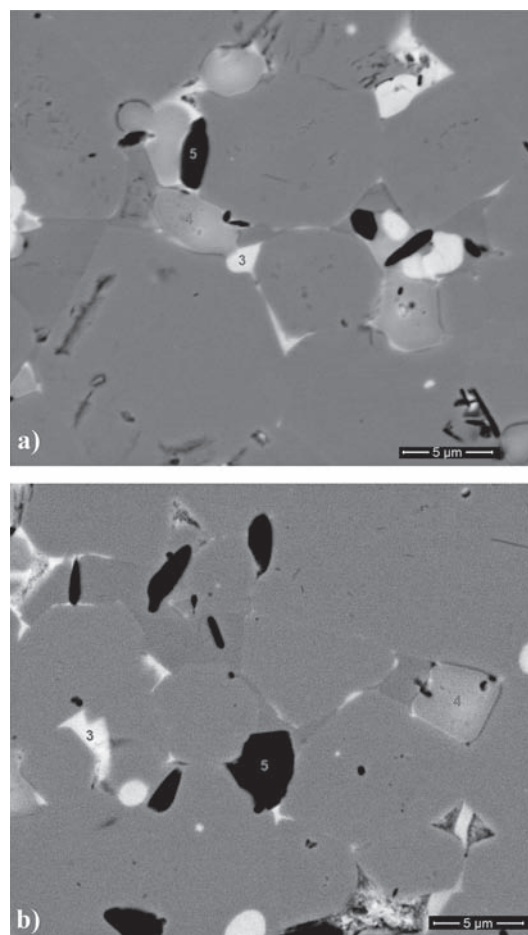
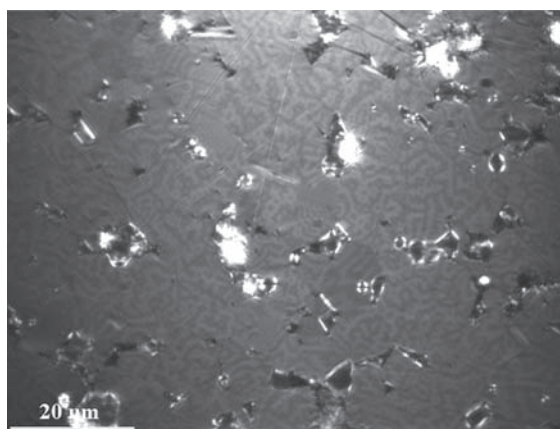
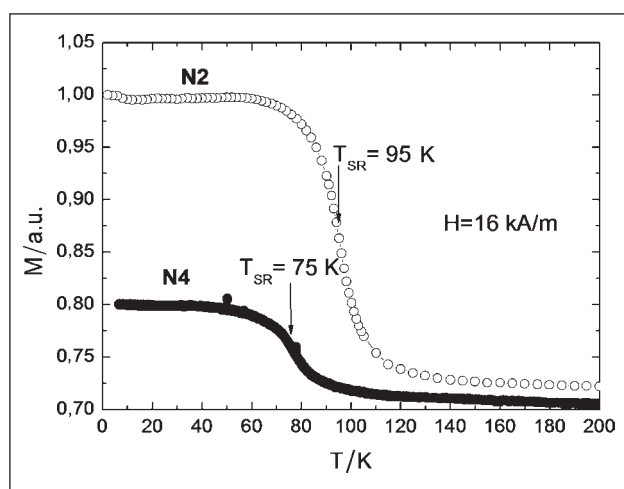


Figure 1 SEM images of the microstructure of sintered magnets with a) 10 wt. % Pr (sample N2) and b) 13 wt. % Pr (sample N4).



**Figure 2** Domain structure of the magnet with 10 wt. % Pr (in the thermally demagnetized state) observed on the surface perpendicular to the magnet texture.



**Figure 3** The temperature dependence of magnetization measured in a magnetic field of 16 kA/m for the samples of permanent magnets N2 and N4, having optimal heat treatment.

$\text{Nd}(\text{Pr})\text{O}_2$  or  $(\text{Nd},\text{Pr})_2\text{O}_3$  oxides present at grain triple junctions (points 4.1 and 4.2) and Ti-based phase (point 5). According to the EDX microanalysis data in Table 2, the composition of the matrix grains corre-

sponds to the  $(\text{Pr}_{0.3}\text{Nd}_{0.7})\text{Fe}_{14}\text{B}$  and  $(\text{Pr}_{0.4}\text{Nd}_{0.6})\text{Fe}_{14}\text{B}$  for the magnets with 10 and 13 wt. % Pr, respectively.

According to the literature data [5], the temperature of spin-reorientation transition for the compositions is 93 and 75 K, respectively. We performed thermal magnetic analysis of the permanent magnets subjected to optimum heat treatment (samples N2 and N4). According to the measured temperature dependences of magnetization (Figure 3), the determined spin-reorientation transition temperatures agree well with those available in the literature. This is due to the fact that the temperature is determined by the chemical composition of grains.

Figure 2 shows the domain structure of the magnet with 10 wt. % Pr (sample N2). The domain structure was observed from the plane perpendicular to the texture axis; it is typical of the basal plane of uniaxial hard magnetic materials [12]. This fact indicates the adequate magnetic texture of the magnets. The closeness of the  $H_k$  and  $H_{cj}$  magnitudes of the magnets (see Table 1) confirms the adequate magnetic texture of the magnet.

## CONCLUSIONS

The stoichiometric composition of the matrix grains in the  $(\text{Nd}, \text{Pr})\text{-Fe-B}$  magnets with 10 and 13 wt. % Pr corresponds to  $(\text{Pr}_{0.3}\text{Nd}_{0.7})\text{Fe}_{14}\text{B}$  and  $(\text{Pr}_{0.4}\text{Nd}_{0.6})\text{Fe}_{14}\text{B}$  compounds, respectively. Conducted thermomagnetic analysis to samples of these magnets showed the presence of spin-reorientation transition in temperature 95 and 75 K, respectively. The latter composition has the spin-reorientation transition temperature close to the liquid-nitrogen boiling temperature and it can be recommended for low-temperature applications.

The heat treatment of the magnets for the high-coercivity state consists in the 2-h vacuum annealing at 500 °C.

The observed domain structure of the magnet with 10 wt. % Pr and the closeness of the  $H_k$  and  $H_{cj}$  magnitudes indicate the adequate magnetic texture of the magnets.

**Table 3** Chemical analysis of individual phases observed in the magnet structure in / at. %.

| Sample | Point | O     | Dy   | Al   | Nb   | Ti    | Pr    | Nd    | Fe    | Co   | Cu   |
|--------|-------|-------|------|------|------|-------|-------|-------|-------|------|------|
| N2     | 1     | 6,34  | 0,23 | 1,22 | 0,12 | 0,35  | 4,00  | 9,56  | 77,02 | 0,60 | 0,59 |
|        | 2     | 6,65  | 0,57 | 0,22 | 0,20 | 0,48  | 6,80  | 15,70 | 68,11 | 0,52 | 0,76 |
|        | 3     | 8,26  | 0,99 | 1,77 | 0,07 | 0,52  | 15,87 | 27,64 | 39,86 | 0,34 | 4,70 |
|        | 4.1   | 50,54 | 0,83 | 0,11 | 0,21 | 1,44  | 15,23 | 25,91 | 4,00  | 1,02 | 0,71 |
|        | 4.2   | 59,63 | 0,70 | 0,00 | 0,10 | 0,54  | 12,03 | 24,34 | 1,86  | 0,33 | 0,49 |
|        | 5     | 13,33 | 0,45 | 0,47 | 0,18 | 63,72 | 2,24  | 4,53  | 14,46 | 0,19 | 0,43 |
| N4     | 1     | 6,65  | 0,12 | 1,47 | 0,13 | 0,31  | 5,50  | 8,08  | 76,94 | 0,42 | 0,38 |
|        | 2     | 7,37  | 0,27 | 0,48 | 0,22 | 0,56  | 8,89  | 12,49 | 68,75 | 0,56 | 0,42 |
|        | 3     | 7,94  | 0,38 | 5,99 | 0,16 | 0,43  | 14,77 | 15,46 | 53,18 | 0,57 | 1,16 |
|        | 4.1   | 50,48 | 0,00 | 0,09 | 0,26 | 1,00  | 15,17 | 18,05 | 13,50 | 0,65 | 0,78 |
|        | 4.2   | 63,86 | 0,51 | 0,20 | 0,17 | 1,48  | 13,56 | 16,84 | 2,29  | 0,41 | 0,68 |
|        | 5     | 5,08  | 0,10 | 0,37 | 0,05 | 82,39 | 0,90  | 0,96  | 9,26  | 0,35 | 0,54 |

## Acknowledgement

This paper was created within the project No. LO1203 „Regional Materials Science and Technology Centre – Feasibility Program” funded by the Ministry of Education, Youth and Sports of Czech Republic. The research was also supported by the NCBR (Poland) and FASIE (Russia) within the project “ERA.Net RUS Plus: No. 146-MAGNES” financed by the EU 7<sup>th</sup> FP, grant no 609556.

## REFERENCES

- [1] C. Benabderrahmane, P. Berteaud, M. Valle´au, C. Kitegi, K. Tavakoli, N.Be´chu, A. Mary, J.M. Filhol, M.E. Couprie, Nd<sub>2</sub>Fe<sub>14</sub>B and Pr<sub>2</sub>Fe<sub>14</sub>B magnets characterization and modelling for cryogenic permanent magnet undulator applications, *Nuclear Instruments and Methods in Physics Research A* 669 (2012) 1-6.
- [2] J. F. Herbst, R<sub>2</sub>Fe<sub>14</sub>B materials: Intrinsic properties and technological aspects, *Reviews of Modern Physics* 63 (1991) 4 819-898. DOI: 10.1103/RevModPhys.63.819.
- [3] Z. Lin, J. Han, S. Liu, M. Xing, Y. Zhang, C. Wang, J. Yang and Y. Yang, Coercivity enhancement in anisotropic Pr<sub>13</sub>Fe<sub>79.4</sub>B<sub>7</sub>Nb<sub>0.7</sub>Ga<sub>0.3</sub> powders, *Journal of Applied Physics* 111 (2012) 7 07A722. DOI: 10.1063/1.3677664.
- [4] J. Ni, M. Yan, T. Ma, W. Zhang, Magnetic and anticorrosion properties of two-powder (Pr, Nd)<sub>12.6</sub>Fe<sub>81.3</sub>B<sub>6.1</sub>-type sintered magnets with additions of (Pr, Nd)<sub>32.5</sub>Fe<sub>62.0</sub>Cu<sub>55</sub>, *Materials Chemistry and Physics* 151 (2015) 1 126-132. DOI: 10.1016/j.matchemphys.2014.11.046.
- [5] Y. Yu, J. Hanmin, Y.B. Kim, Crystal field analysis of magnetization curves for aligned (Pr,Nd)<sub>2</sub>Fe<sub>14</sub>B, *Journal of Magnetism and Magnetic Materials* 221 (2000) 3 382-390. DOI: 10.1016/S0304-8853(00)00512-6.
- [6] K. Uestuener, M. Katter, R. Blank, D. Benedikt, J. Bahrtdt, A. Gaupp, et al., Sintered (Pr,Nd)-Fe-B permanent magnets with (BH)<sub>max</sub> of 520 kJ/m<sup>3</sup> at 85 K for cryogenic applications, In Proc. 20<sup>th</sup> Int. Workshop on Rare Earth Permanent Magnets & Their Applications, ed. by D. Niarchos, Knossos (2008) 397-400.
- [7] C. Brombacher, K. Uestuener, F.-J. Boergermann, M. Katter, Grain-boundary diffusion of Pr-Fe-B magnets for cryogenic applications, In Proc. 23<sup>rd</sup> Int. Workshop on Rare Earth Permanent Magnets & Their Applications, Annapolis, Maryland (2014) 339-341.
- [8] O.A. Arinicheva, A.S. Lileev, M. Reissner, A.A. Lukin, A.S. Starikova, Magnetic and microstructural properties of (Nd,Pr)-(Tb,Dy,Gd)-(Fe,Co,Al,Cu)-B type magnets, *Hyperfine Interactions* 219 (2013) 1 89-93. DOI: 10.1007/s10751-012-0738-9.
- [9] N. Kolchugina, A. Lukin, G.S. Burkhanov, K. Skotnicová, H. Drulis, V. Petrov, Role of terbium hydride additions in the formation of microstructure and magnetic properties of sintered Nd-Pr-Dy-Fe-B magnets, In *Metal 2012: 21<sup>th</sup> International Conference on Metallurgy and Materials*. May 23<sup>rd</sup>-25<sup>th</sup> 2012 Brno, Czech Republic (2012) 1387-1392. WOS: 000318506500215.
- [10] Y.S. Koshkid'ko, K.Skotnicová, M. Kursá, T. Čegan, G.S. Burkhanov, N.B. Kolchugina, A. A. Lukin, A.G. Dormidontov, V.V. Sitnov. The effect of heat treatment under various conditions on microstructure of sintered (Nd,Pr,Dy)-Fe-B magnets. In *METAL 2014: 23<sup>rd</sup> International Conference on Metallurgy and Materials*, Conference Proceedings May 21<sup>nd</sup>-23<sup>rd</sup> 2014 Brno, Czech Republic (2014) 1369-1374. WOS: 000350641700227.
- [11] J. Malcharczikova, M. Kursá, Structural characteristics of Ni<sub>3</sub>Al based alloys depending on the preparation conditions, *Metalurgija* 54 (2015) 4 635-638.
- [12] Yu.G. Pastushenkov, A. Forkl, H. Kronmüller, Temperature dependence of the domain structure in Fe<sub>14</sub>Nd<sub>2</sub>B single crystals during the spin-reorientation transition, *Journal of Magnetism and Magnetic Materials* 174 (1997) 3 278-288. DOI: 10.1016/S0304-8853(97)00198-4.

**Note:** The translator responsible for English language is B. Škandera, Czech Republic